Supplements to: Nature and origin of variations in pelagic carbonate production in the tropical ocean since the Mid Miocene (ODP Site 927)

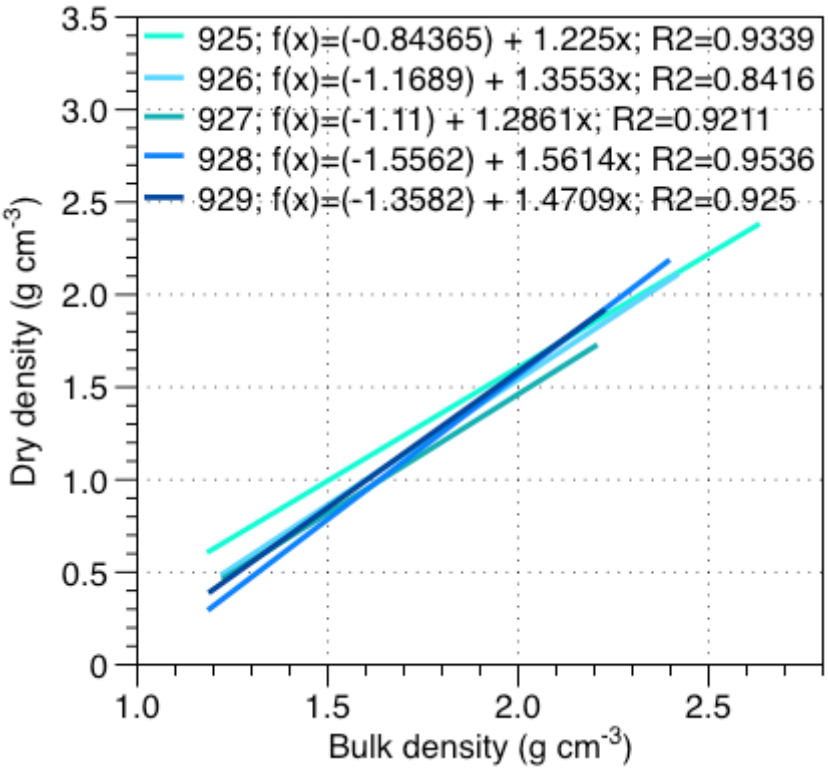

Figure S1. Regression curves for the gamma-ray attenuation (GRA) bulk density and DBD using data from Curry et al. (1995) for the five cores of the Leg 154.

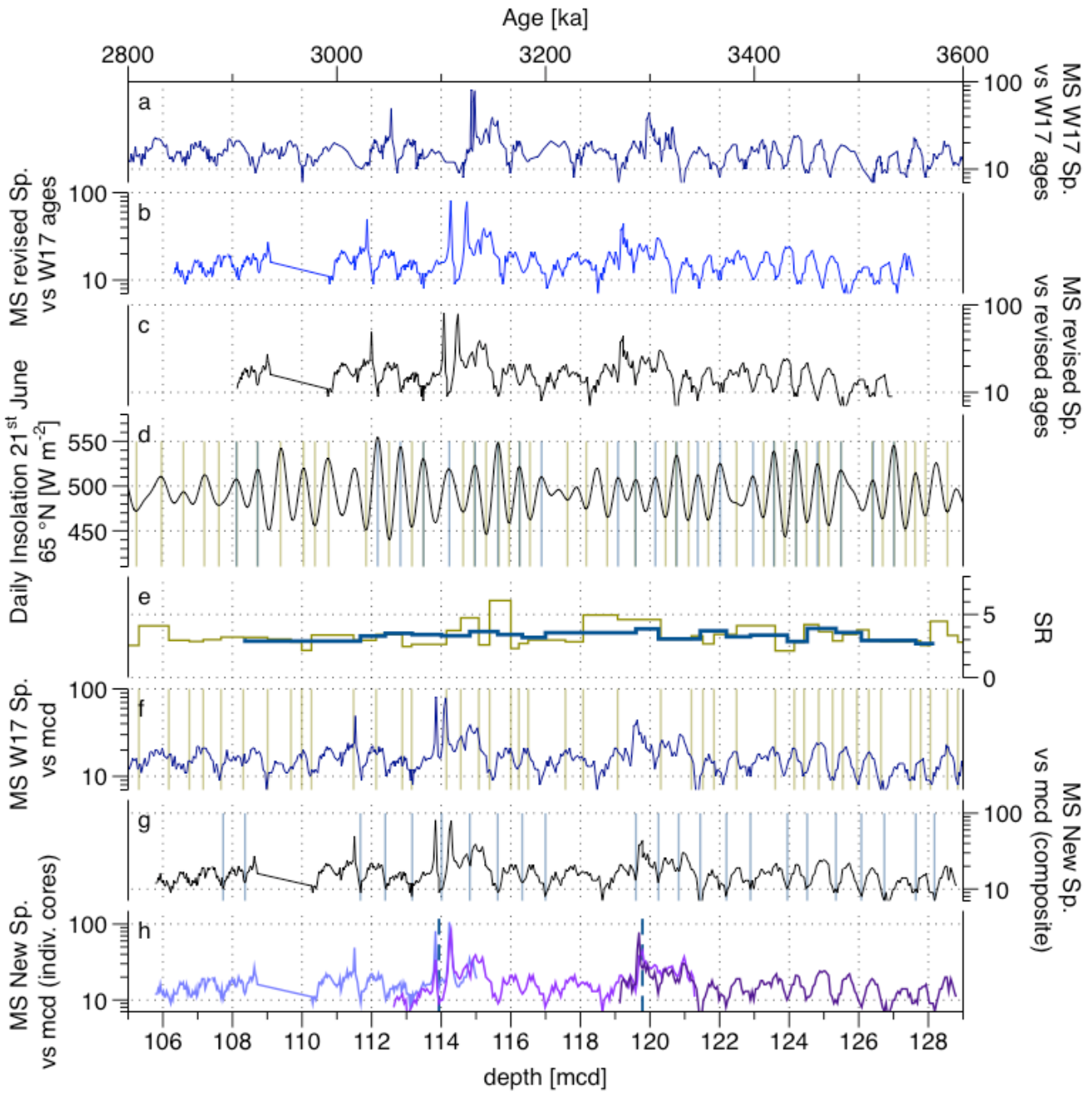

Figure S2. Comparison of the magnetic susceptibility (MS) records according to the different composite depths and age-model options for the Pliocene interval of this study. a) MS record versus age (Wilkens et al., 2017); b) MS record following the revised splice (Sect. 3.2.2) versus Wilkens et al. (2017) ages; c) MS record following the revised splice (Sect. 3.2.2.) versus revised age model ages (Sect. 3.2.2.); d) daily summer insolation 21st of June, 65°N (Laskar et al., 2004), the green lines correspond to the control points ages of Wilkens et al. (2017) age model and the blue lines correspond to the control points ages of the revised age model (Sect. 3.2.2.); e) comparison between the sedimentation rate of Wilkens et al. (2017) age model and the sedimentation rate of the revised age model (Sect. 3.2.2.); f) MS record versus depth (Wilkens et al., 2017), the green lines correspond to the control points composite depth of Wilkens et al. (2017)age model; g) MS record versus revised composite depth (Sect. 3.2.2.), the blue line correspond to the control points composite depths of the revised age model (Sect. 3.2.2.); h) Individual cores MS records versus revised composite depth (Sect. 3.2.2.), the blue dash lines correspond to the depths we switch from one individual core section to the other in the composite splice.

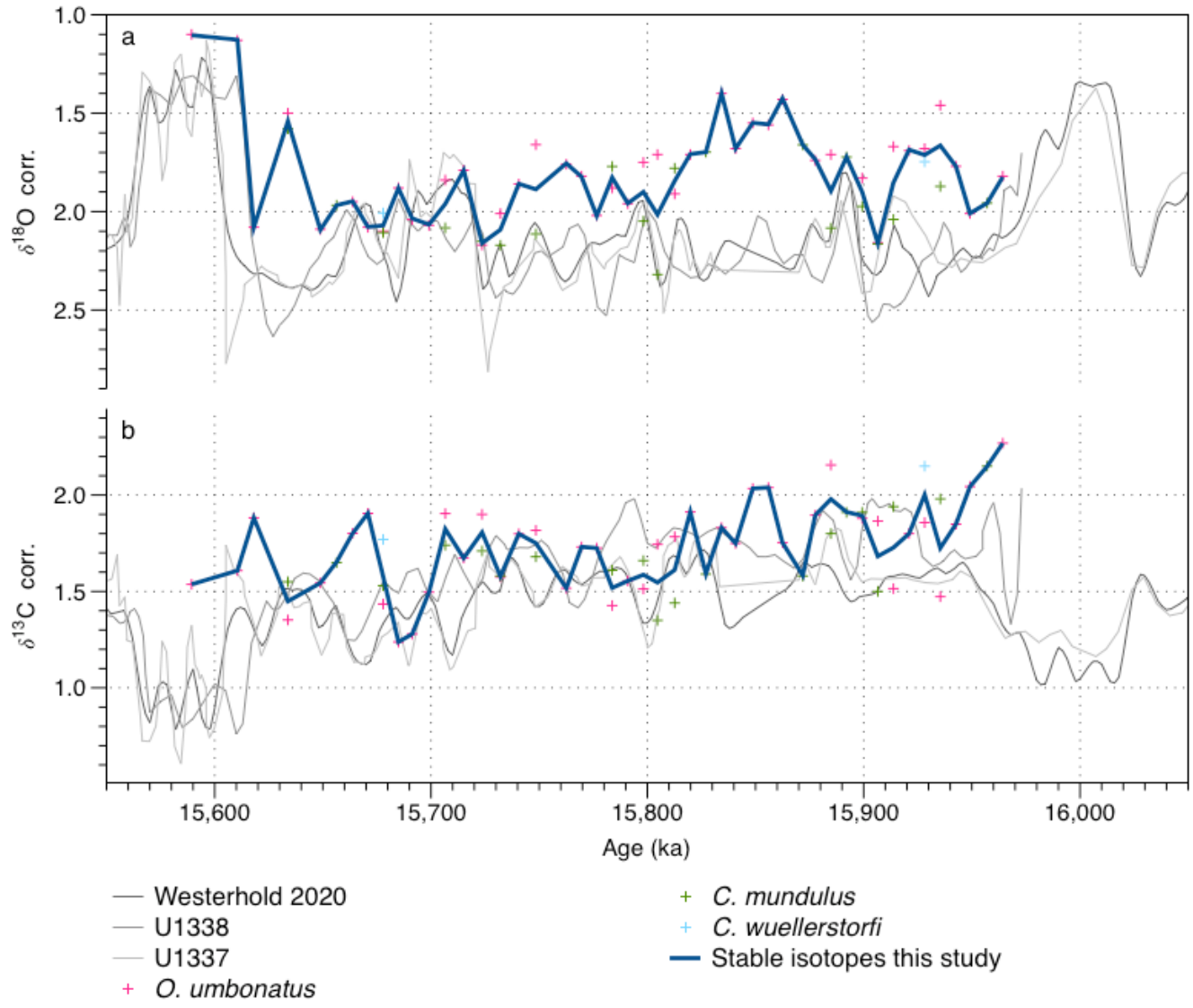

25

Figure S3. Stable isotopes analyses species-specific corrected and average record from this study compared to the stable isotopes loess smooth record (Westerhold et al., 2020) and stable isotopes record of sites U1338 and U1337 (Lyle et al., 2019) for both a) the $\delta^{18}O$ and b) the $\delta^{13}C$.

30